



# LABORATORY WAVE MEASUREMENTS ON TOYOURA SAND AND HIME GRAVEL

Ruta Ireng WICAKSONO<sup>1</sup>, Yukika TSUTSUMI<sup>2</sup>, Takeshi SATO<sup>3</sup>, Junichi KOSEKI<sup>4</sup>, and Reiko KUWANO<sup>5</sup>

**ABSTRACT:** A triaxial test apparatus combined with two independent wave measurement methods, i.e. Trigger Accelerometer and Bender Element, was employed. A series of tests were conducted to the specimens of Toyoura sand and Hime gravel. Analyses were performed on the test results to obtain statically and dynamically measured moduli. The values of shear modulus resulted from static measurement, Trigger Accelerometer, and Bender Element methods were compared at different isotropic stress levels. The effects of specimen size on static and dynamic measurements were studied. It was confirmed that the void ratio function proposed by Hardin and Richart (1963) is the most appropriate among others for Toyoura sand and Hime gravel. In addition, strain level estimation during dynamic measurements was evaluated.

**Key Words:** Trigger Accelerometer, Bender Element, void ratio function, strain level estimation

## INTRODUCTION

In the past, dynamic measurements regarding wave velocity analysis, based on the cross-hole and down-hole methods, have been used for a long time in real construction sites (Stokoe & Hoar, 1978). Recently measurement of wave velocities in the laboratory has also become popular, and researchers have recognized that “dynamic” and “static” properties are no more different from each other except for the strain levels (Woods, 1991). Precise static small strain measurements in the laboratory tests have bridged the gap of strain levels between “dynamic” and “static” behavior (Tatsuoka and Shibuya, 1992). However, following the pioneer work by Tanaka et al. (2000), AnhDan and Koseki (2002) found that the difference on dynamic and static properties is not only caused by strain level but also by some other factors like grain size and wave length.

Among many laboratory tests with dynamic measurements based on elastic wave propagation, this study focused on two independent wave measurement methods in a series of triaxial tests, i.e. Trigger-Accelerometer (TA) method and Bender Element (BE).

## MATERIAL, APPARATUS, AND TEST PROCEDURES

Air-dried Toyoura sand ( $G_s=2.635$ ,  $e_{max}=0.966$ ,  $e_{min}=0.600$ ,  $D_{50}=0.20$  mm) and Hime gravel ( $G_s=2.650$ ,  $e_{max}=0.709$ ,  $e_{min}=0.480$ ,  $D_{50}=1.72$  mm) were used as the test material. The material particles were

---

<sup>1</sup> Graduate Student

<sup>2</sup> Technical Staff

<sup>3</sup> Research Support Promotion Member

<sup>4</sup> Professor

<sup>5</sup> Associate Professor

pluviated through air to prepare cylindrical specimens. As the initial condition, the specimens were consolidated with a confining stress ( $\sigma_c'$ ) of 25 kPa in the air-pressured cell. Twenty tests of those geomaterials having different dry densities ( $\rho$ ) were performed as presented in Table 1.

Table 1. List of the tested specimens

| Test No. | Material     | Dry density, $\rho_d$<br>(gram/cm <sup>3</sup> ) | Specimen Size<br>[dia. (cm); height (cm)] |
|----------|--------------|--|---|
| T1       | Toyoura sand | 1.458  | 5 ; 10                                    |
| T2       | Toyoura sand | 1.590  | 5 ; 10                                    |
| T3       | Toyoura sand | 1.533  | 5 ; 10                                    |
| T4       | Toyoura sand | 1.595  | 5 ; 10                                    |
| T5       | Toyoura sand | 1.597  | 5 ; 10                                    |
| T6       | Toyoura sand | 1.602  | 5 ; 10                                    |
| T7       | Toyoura sand | 1.604  | 5 ; 10                                    |
| T8       | Toyoura sand | 1.603  | 10 ; 20                                   |
| T9       | Hime gravel  | 1.743  | 10 ; 20                                   |
| T10      | Hime gravel  | 1.737  | 10 ; 20                                   |
| T11      | Hime gravel  | 1.762  | 5 ; 10                                    |
| T12      | Hime gravel  | 1.736  | 5 ; 10                                    |
| T13      | Hime gravel  | 1.731  | 5 ; 10                                    |
| T14      | Hime gravel  | 1.741  | 5 ; 10                                    |
| T15      | Hime gravel  | 1.722  | 5 ; 10                                    |
| T16      | Hime gravel  | 1.733  | 5 ; 10                                    |
| T17      | Hime gravel  | 1.756  | 5 ; 10                                    |
| T18      | Hime gravel  | 1.682  | 5 ; 10                                    |
| T19      | Hime gravel  | 1.571  | 5 ; 10                                    |
| T20      | Hime gravel  | 1.577  | 5 ; 10                                    |

The triaxial test apparatus was used for this study. To evaluate dynamic measurement based on elastic wave propagation, two independent wave measurement methods were employed, i.e. Trigger Accelerometer (TA) and Bender Element (BE). Triggers and accelerometers were combined to observe the wave propagation through the specimens using P and S waves (AnhDan et al. 2002). On the other hand, only S wave was employed during dynamic measurement with BE. Photo and schematic figure of Trigger Accelerometer (TA) and Bender Element (BE) methods are presented in Figure 1.

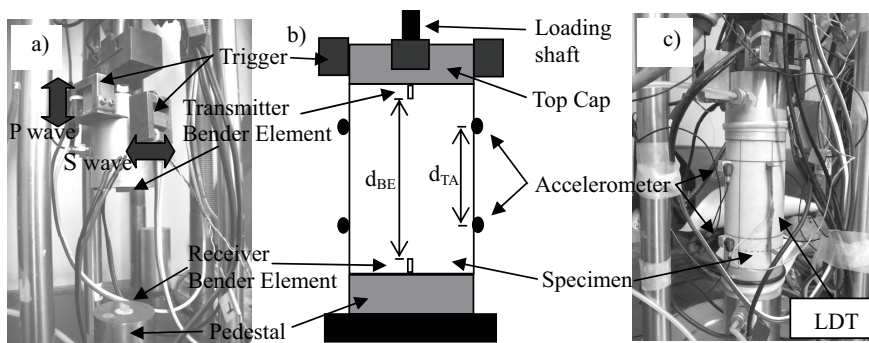


Figure 1. Specimen, Trigger Accelerometer, and Bender Element

In evaluating elastic wave velocities, the wave form is one of the crucial factors. To obtain relatively better wave measurement, some improvements were performed including modification on manner of attaching accelerometer in TA method and replacing cables/connectors in BE method

(Wicaksono, 2007).

Starting from a confining stress ( $\sigma_c'$ ) of 25 kPa, the isotropic stress levels were increased to 50 kPa, 100 kPa, 200 kPa, and 400 kPa. At each stress level, after a 10 minute stage with constant stress state, 11 cycles of vertical loading with a single axial strain amplitude of about 0.002% measured by Local Deformation Transducer, LDT (Fig.1c), were carried out as a static measurement. During the cyclic loading stage, the vertical stress was unloaded first then reloaded to the original stress level under drained condition. After completing the cyclic loading, another stage with constant stress state was maintained while conducting the dynamic measurement using TA and BE methods.

### PROCEDURES FOR ANALYZING TEST RESULT

In order to evaluate quasi-elastic stiffness modulus based on static measurement, data of the fifth and the tenth cycles among 11 cyclic loading were analyzed. A typical result is shown in Figure 2, where increments of the vertical strain and stress were detected with LDTs and the load cell, respectively. The stress-strain relationship was fitted by a straight line and the quasi elastic vertical Young's modulus ( $E_s$ ) was evaluated from the slope of the line.

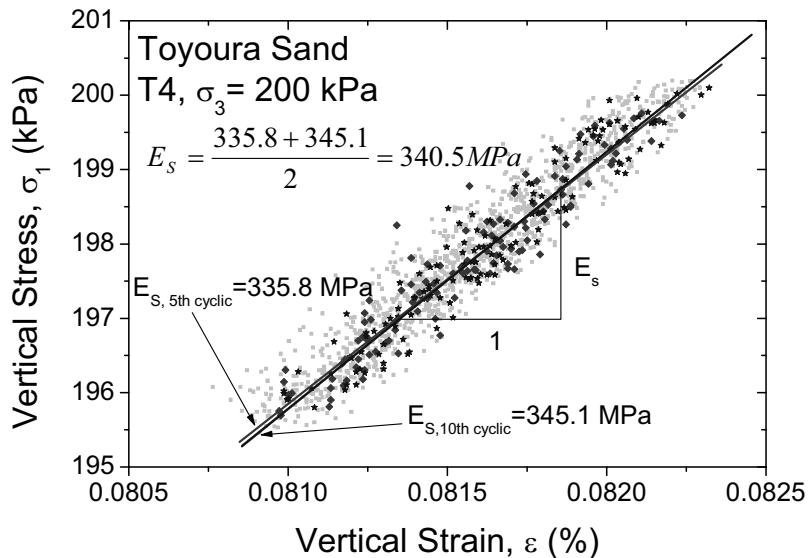


Figure 2. Analyzing Young's Modulus resulted from cyclic loading

In the dynamic measurement analysis, a wave velocity ( $V$ ) was evaluated using Equation (1), as follows:

$$V = \frac{d}{t} \quad (1)$$

where  $d$  is the effective distance between two sensors/transducers as shown in Figure 1b, where  $d_{TA}$  and  $d_{BE}$  are the effective distance between 2 accelerometers and 2 bender elements, respectively. Meanwhile,  $t$  is the travel time (i.e. the time difference between input and output waves). In this study, input wave is the wave which is captured by upper accelerometer (Figure 1b) or is recorded by

transmitter BE. Output wave is the wave which is captured by lower accelerometer (Figure 1b) or receiver BE.

In wave velocity evaluation, the determination of travel-time plays an important role, considering the fact that it often depends on subjective interpretation of each researcher. In this study, to avoid the uncertainties and the unreliable wave forms while computing wave velocity, the travel-time values evaluated with sinusoidal excitation and rising-to-rising technique employing both the TA and the BE methods, were used. As shown in Figure 3 as a typical definition used in TA and BE methods, the rising-to-rising travel time is defined as a distance at time-history-axis from a point obtained after applying a zero-crossing line at the first input-signal to a point obtained after applying zero-crossing line at the first output-signal. The zero-crossing line is applied to correct for the near field effect.

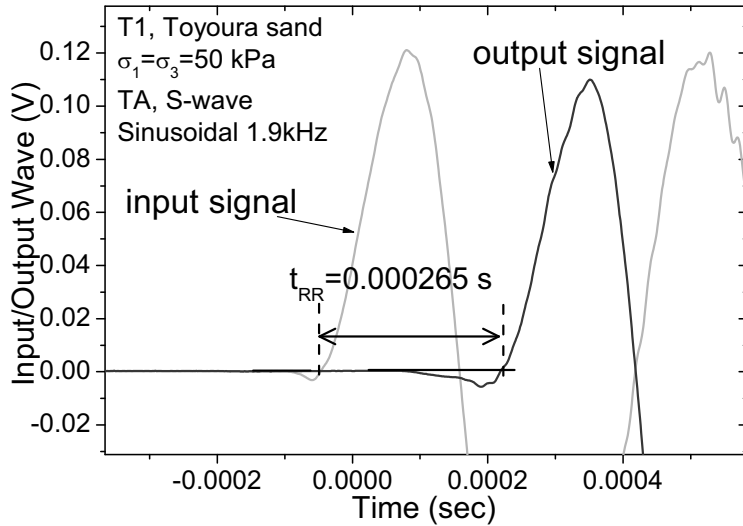


Figure 3. Definition and Evaluation of travel time

By knowing density of the specimen ( $\rho$ ), the soil stiffness can be obtained. Since Primary (P) and Secondary (S) waves are employed, both dynamic Young's modulus ( $E_D$ ) under unconstrained condition and dynamic shear modulus ( $G_D$ ) can be evaluated using Equation (2) and Equation (3) respectively, as follows:

$$E_D = \rho \cdot V_P^2 \quad (2)$$

$$G_D = \rho \cdot V_S^2 \quad (3)$$

where  $V_P$  and  $V_S$  are wave velocities corresponding to P and S waves, respectively.

In addition, to compare the values of moduli resulted from static and dynamic measurements in this study, the dynamic Young's modulus ( $E_D$ ) and the static Young's modulus ( $E_s$ ) were converted to the dynamic shear modulus ( $G_D$ ) and the statically measured shear moduli ( $G_{sta}$ ) using Equation (4) and Equation (5), respectively, under isotropic assumption as follows:

$$G_D = \frac{E_D}{2(1+\nu)} \quad (4)$$

$$G_{sta} = \frac{E_s}{2(1+\nu)} \quad (5)$$

where  $\nu$  is Poisson's ratio. The values of Poisson's ratio were set as 0.17 (Hoque, 1996) and 0.20 (De Silva, 2004) for Toyoura sand and Hime gravel, respectively.

Void ratio function was used to compare the quasi-elastic deformation properties among specimen with different void ratios. Following are some of the widely used void ratio functions.

$$f(e) = \frac{(2.17 - e)^2}{(1 + e)} \quad (\text{Hardin and Richart, 1963}) \quad (6)$$

$$f(e) = \frac{(2.97 - e)^2}{(1 + e)} \quad (\text{Hardin and Richart, 1963}) \quad (7)$$

$$f(e) = \frac{(7.32 - e)^2}{(1 + e)} \quad (\text{Kokusho et al, 1985}) \quad (8)$$

$$f(e) = \frac{1}{e^{1/3}} \quad (\text{Jamiolkowski et al, 1991}) \quad (9)$$

$$f(e) = e^{-2.4} \quad (\text{Shibuya et al, 1997}) \quad (10)$$

In this study, the applicability of the entire above mentioned void ratio functions was checked by plotting Equation (11) on the graph, as follows:

$$G = \frac{G_{o(ref)}}{f(e)_{o(ref)}} f(e) \quad (11)$$

where  $G_{o(ref)}$  is reference shear modulus, and  $f(e)_{o(ref)}$  is reference void ratio function of the respective  $f(e)$  considering  $G_{o(ref)}$ .

Estimation of the maximum strain associated with the elastic wave velocity measurement was evaluated. By assuming that the element tip deflections of the BE are equivalent to the soil particle vibration, the particle velocity,  $\dot{y}(t)$ , can be estimated from the time history of the free deflection of BE  $[x_f(t)]$  using Equation (12) and Equation (13) for series and parallel type of BE respectively, as follows:

$$\dot{y}(t) = \dot{x}_f(t) = \frac{3}{2} d_{31} \left( \frac{l_b}{T} \right)^2 \left( 1 + \frac{t_s}{T} \right) \dot{V}(t) K \quad (12)$$

$$\dot{y}(t) = \dot{x}_f(t) = 3 d_{31} \left( \frac{l_b}{T} \right)^2 \left( 1 + \frac{t_s}{T} \right) \dot{V}(t) K \quad (13)$$

where  $d_{31}$  is the piezoelectric strain constant,  $l_b$  is the protrusion length of the Bender Element,  $t_s$  is thickness of the center shim (for parallel type),  $T$  is the thickness,  $\dot{V}(t)$  is the voltage rate, and  $K$  is an empirical weighting factor ( $\geq 1$ ). For the Bender Element used in this study,  $d_{31} = -210 \times 10^{-12}$  m/V,  $t_s$

= 0.05 mm, and  $K = 2$  (Fuji Ceramics Corp, 2002). The shear strain ( $\gamma$ ) were estimated using Equation (14) (White, 1965) as follows:

$$\gamma = \frac{\dot{y}_{\max}}{V_s} \quad (14)$$

where  $\dot{y}_{\max}$  is the maximum particle velocity and  $V_s$  is the wave velocity of the corresponding signal.

In the case with the TA method, the shear strain ( $\gamma$ ) was estimated using equation (14) as well, which the  $\dot{y}_{\max}$  value was evaluated using Equation (15d) as follows:

$$y = y_o \sin(2\pi ft) \quad (15a)$$

$$\dot{y} = (2\pi f)y_o \cos(2\pi ft) \quad (15b)$$

$$\ddot{y} = -(2\pi f)^2 y_o \sin(2\pi ft) \quad (15c)$$

$$\dot{y}_{\max} \cong \frac{\ddot{y}_{\max}}{2\pi f} \quad (15d)$$

where  $y$  is the amplitude of wave,  $f$  is the frequency of wave ( $=V_s/\lambda$ ),  $t$  is time history, and  $\ddot{y}_{\max}$  is the maximum acceleration of the wave that was measured by the accelerometer.

## TEST RESULTS AND DISCUSSIONS

Figure 4 shows typical graphs of comparison between static and dynamic moduli of Toyoura sand at different isotropic stress states under dry and saturated conditions, respectively. Hereafter, the values of shear modulus under dry and saturated conditions are plotted on the graph with solid and hollow symbols, respectively.

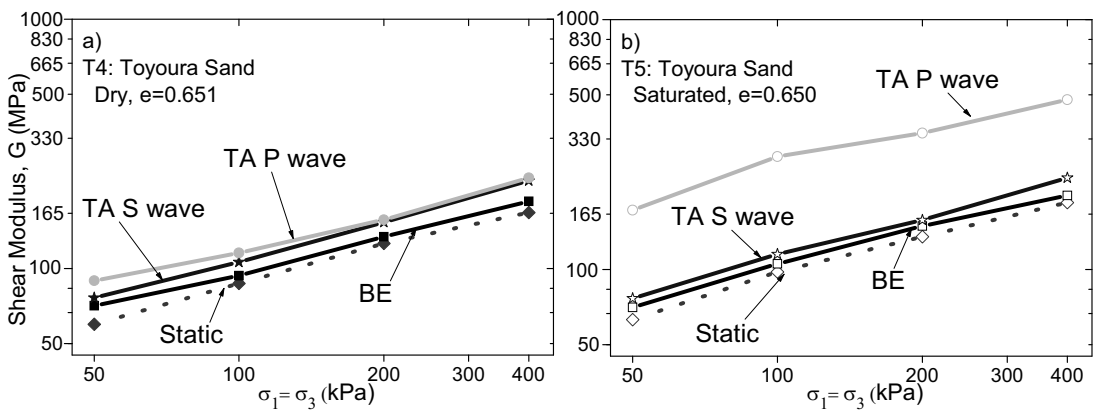


Figure 4. The values of shear moduli on Toyoura sand

As shown in Figure 4a and 4b for under dry and saturated conditions respectively, the values of dynamic shear modulus with the BE ( $G_{D,BE}$ ) and the value of the statically measured shear modulus ( $G_{sta}$ ) on Toyoura sand are compared. The values of  $G_{D,BE}$  were at largest 20% larger than those of  $G_{sta}$ . Similar tendency was observed between the specimens under dry and saturated conditions. Under dry condition, the values of the dynamic shear modulus with TA method using S wave ( $G_{D,TA-S}$ ) were 15% - 50% larger than those of  $G_{sta}$ , while the values of dynamic shear modulus with TA method using P wave ( $G_{D,TA-P}$ ) were 20% - 70% larger than those of  $G_{sta}$ . Under saturated condition, the values of  $G_{D,TA-S}$  showed the tendency that was similar to those observed under dry condition. On the other hand, the values of  $G_{D,TA-P}$  were significantly larger than those of  $G_{sta}$  under saturated condition. The values of  $G_{D,BE}$  were larger than those of  $G_{sta}$ , but were smaller than those of  $G_{D,TA-S}$ .

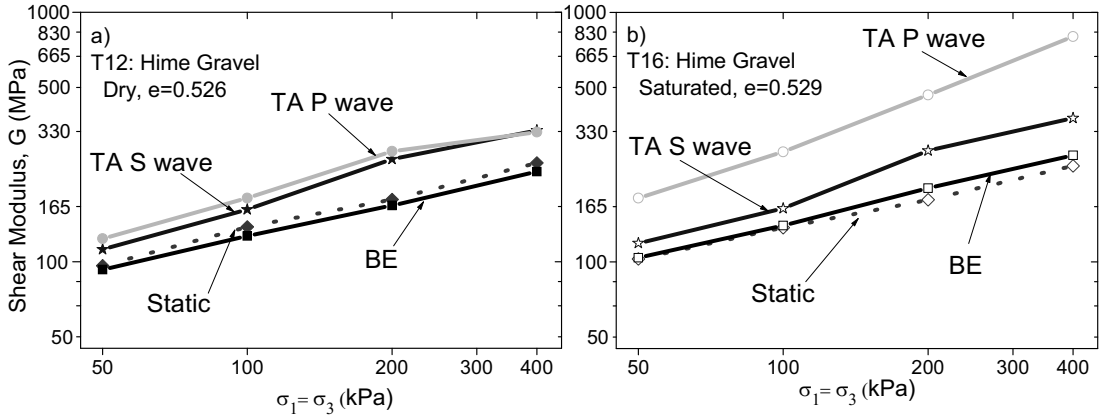


Figure 5. The values of shear moduli on Hime gravel

For Hime gravel as shown Figure 5, at smallest 20% smaller the values of  $G_{D,BE}$  as compared to those of  $G_{sta}$  were observed under dry condition. While under saturated condition, as shown in Fig. 14b the  $G_{D,BE}$  values were close to  $G_{sta}$ . Similarly to the case with Toyoura sand, for Hime gravel as shown in Fig. 16 the values of  $G_{D,TA-P}$  under dry condition, and as well, the values of  $G_{D,TA-S}$  both under dry and saturated conditions were larger than those of  $G_{sta}$  with relatively having the same ratio. Meanwhile, the values of  $G_{D,TA-P}$  under saturated condition were significantly larger than those of  $G_{sta}$ .

Comparison on different specimen sizes of Toyoura sand and Hime gravel were evaluated as shown in Figure 6. Small specimen was represented by specimen size of 5 cm in diameter and 10 cm height, while the large one was represented by that of 10 cm in diameter and 20 cm height. In Figure 6a, the values of  $G_{sta}$  and  $G_{D,TA-P}$  between those resulted by large and small specimens large specimens for Toyoura sand were compared. Meanwhile in Figure 6b, the values of  $G_{sta}$ ,  $G_{D,TA-S}$ , and  $G_{D,TA-P}$  between those resulted by large and small specimens were compared for Hime gravel. In general, those comparison yielded in scattering values of 10%-15% among the respective  $G_{sta}$ ,  $G_{D,TA-S}$ , and  $G_{D,TA-P}$ .

The difference between statically and dynamically measured stiffness moduli is due possibly to the effects of heterogeneity of the specimen. In the static measurement, the stiffness modulus reflects the overall cross-sectional property of the specimen. On the other hand, in the dynamic measurement the wave travels through the shortest path made by interlocking of bigger particles that resulting into larger stiffness modulus as compared to those by the static measurement (Maqbool, 2005).

The difference between two kinds of dynamic shear moduli measured with the TA and the BE methods is due possibly to the effects of bedding error at the interface between the bender element and the specimen at both the top-end and the bottom-end. Gravelly soil yielded in larger size of the locally loose zone at the interface as compared to that with sandy soil seems to result in longer travel time (i.e. smaller dynamic shear modulus) (Wicaksono, 2007).

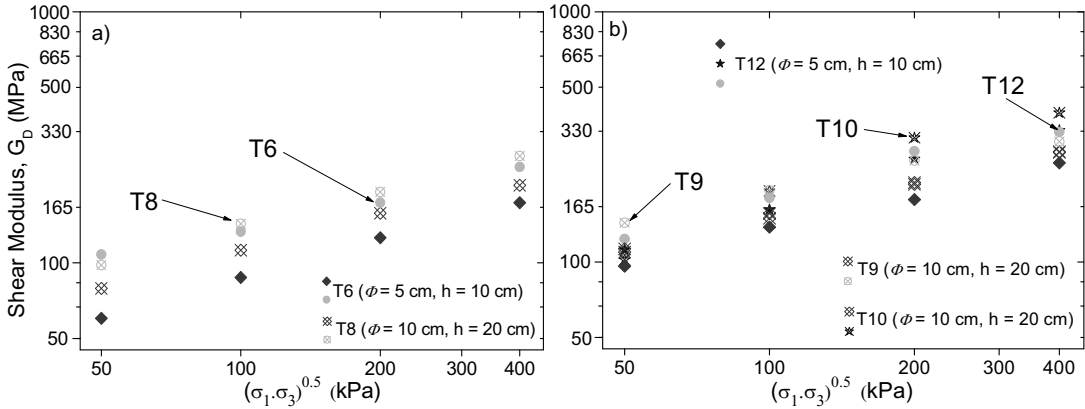


Figure 6. Comparison on specimen sizes

Figure 7 shows the values of shear modulus versus void ratio for Toyoura sand and Hime gravel at isotropic stress state of 100 kPa. By using a reference of a value of  $G_{sta}$  obtained from respective series of data and applying Equation (11) that considers each void ratio function, a line of the function could be plotted. As shown in the figures, the plotted line obtained by applying Equation (6) (Hardin and Richart, 1963) was observed as relatively the fittest function that covering the values of  $G_{sta}$  that was spread over the void ratio ranges of 0.6 – 0.8 for Toyoura sand and of 0.45 – 0.75 for Hime gravel.

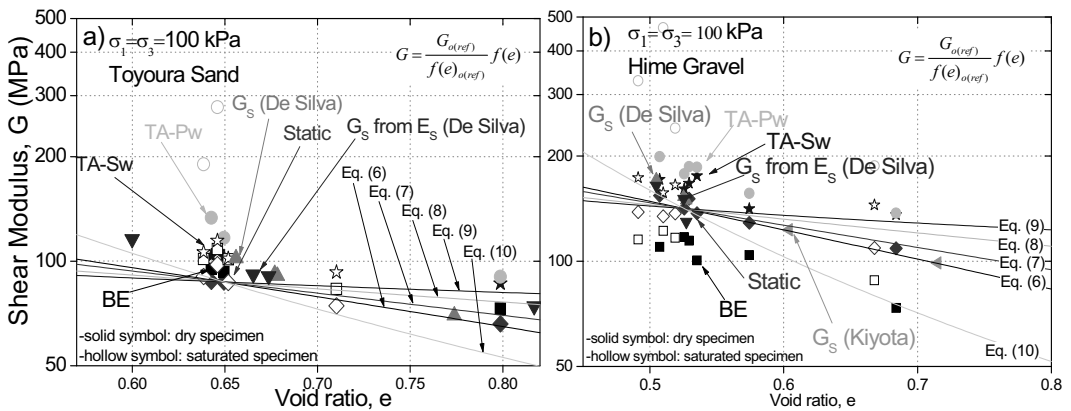


Figure 7. Application of void ratio functions

Figure 8a shows typical graph of the estimation of strain level with the TA method with the S and P waves on Toyoura sand, which was in order of  $10^{-4}\%$ , respectively. Meanwhile, Figure 8b shows estimation of strain level with the BE method on Toyoura Sand. It was found that, in this study the estimated shear strain level with the BE system was in order of  $10^{-3}\%$  at the transmitter and was in order of  $10^{-6}\%$  at the receiver.

Figure 9a shows typical graph of the estimation of strain level with the TA method with the S and P wave excitations on Hime gravel. The estimated shear strain levels were in order of  $10^{-4}\%$  and  $10^{-5}\%$ ,



respectively. Additionally, Figure 9b shows estimation of strain level with the Bender Element method on Hime Gravel. It was found that, in this study the estimated shear strain level with the BE method was in order of  $10^{-3}\%$  at the transmitter and was in order of  $10^{-6}\%$  at the receiver.

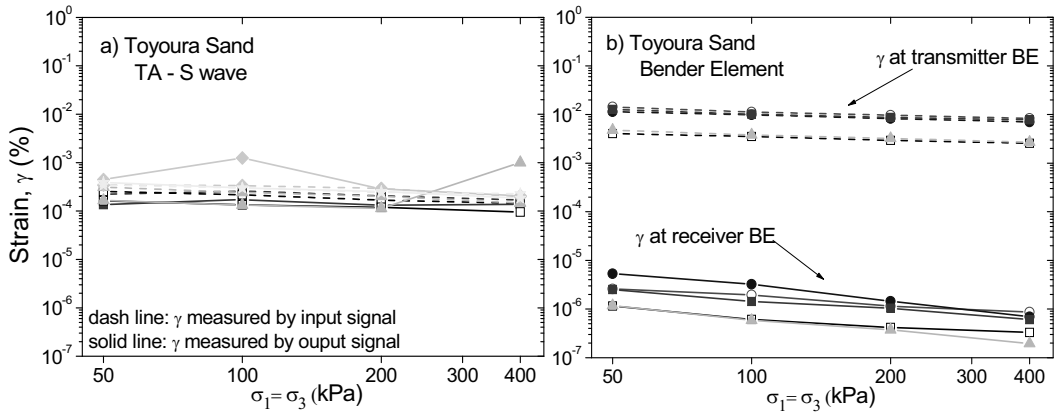


Figure 8. Estimation of strain levels on Toyoura sand

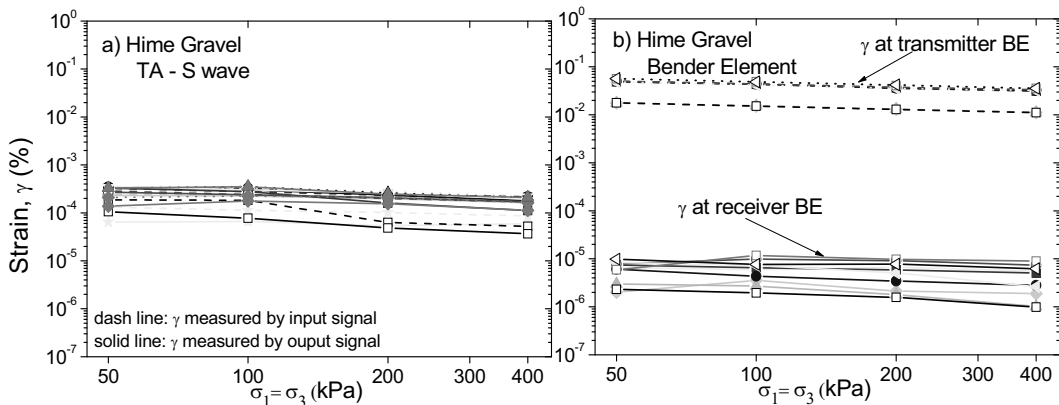


Figure 9. Estimation of strain levels on Hime gravel

Estimation using TA method yielded in relatively the same order of strain level between 2 accelerometers, i.e. lower and upper accelerometers (Figure 1b). Meanwhile using BE method, significant difference of strain levels were observed, due possibly to that strain levels which were evaluated at transmitter BE reflected to the maximum probable strain, while those which were evaluated at receiver BE reflected to likely actual strain.

## CONCLUSIONS

1. The values of shear moduli resulted from dynamic measurements were always larger than those resulted from static measurement, and the values of shear moduli resulted Bender Element method were always smaller than those resulted from Trigger Accelerometer method. In the case

- on Hime gravel, the values of shear moduli resulted from Bender Element method were smaller than those resulted from static measurement, due possibly to bedding error.
2. Effects of specimen size on static and dynamic measurements were observed, which were yielded in scattering values of 10%-15% among the respective shear modulus values.
  3. It was confirmed that the void ratio function proposed by Hardin and Richart (1963) is the most appropriate among others for Toyoura sand and Hime gravel.
  4. Both on Toyoura sand and Hime gravel, the strain level was estimated in the order of  $10^{-4}$ % using Trigger Accelerometer method, while using Bender Element method that was estimated in the order of  $10^{-3}$ % at the transmitter and was in order of  $10^{-6}$ % at the receiver.

## REFERENCES

- AnhDan, L.Q., Koseki, J. and Sato, T. (2002). "Comparison of Young's Moduli of Dense Sand and Gravel Measured by Dynamic and Static Methods," *Geotechnical Testing Journal*, ASTM, Vol. 25 (4), pp. 349-368.
- De Silva, L.I.N. (2004). "Locally Measured Quasi-Elastic Deformation Properties of Geomaterials under Torsional Shear and Triaxial Loadings," Master Thesis, Dept. of Civil Engineering, The University of Tokyo, Japan.
- Fuji Ceramic Corp., 2002, Catalog of Piezoelectric Ceramics.
- Hardin, B.O. and Richart, F.E. (1963). "Elastic Wave Velocities in Granular Soils," *Journal of Soil Mechanics and Foundations*, ASCE, 89 (1). 33-65.
- Hoque, E. (1996). "Elastic Deformation of Sands in Triaxial Tests," PhD. Thesis, University of Tokyo, Japan.
- Jamilowski M., Lancellota, R., Lo Presti, D. C. F. (1995). "Pre-Failure of Geomaterials," Shibuya, Tatsuoka Editors, 817-837.
- Maqbool, S. (2005). "Effects of Compaction on Strength and Deformation Properties of Gravel in Triaxial and Plane Strain Compression Tests," PhD Thesis, Dept. of Civil Engineering, The University of Tokyo, Japan.
- Shibuya, S., Hwang, S. C., Mitachi, T. (1997). "Elastic Shear Modulus of Soft Clays from Shear Wave Velocity Measurements," *Geotechnique*, 47(3), 593-601.
- Stokoe, K.H., II and Hoar, R.J. (1978). "Field Measurement of Shear Wave Velocity by Crosshole and Downhole Seismic Methods," *Proc. of Conf. on Dynamic Methods in Soil and Rock Mechanics*, Karlsruhe, Germany, Vol. 3, pp. 115-137.
- Tanaka, Y., Kudo, K., Nishi, K., Okamoto, T., Kataoka, T. and Ueshima, T. (2000). "Small Strain Characteristics of Soils in Hualien, Taiwan," *Soils and Foundations*, Vol. 40 (3), pp. 111-125.
- Tatsuoka, F. and Shibuya, S. (1992). "Deformation Characteristics of Soils and Rocks from Field and Laboratory Tests," *Proc. of 9th Asian Regional Conf. of SMFE*, Bangkok, Vol. 2, pp. 101-170.
- Wicaksono, R.I., Tsutsumi, Y., Sato, T., Koseki, J. (2006), "Comparison of Different Types of Accelerometers in Wave Velocity Measurement of Toyoura Sand Specimen", *Proc. of 8th IS Symposium*, JSCE, pp. 135-138.
- Wicaksono, R.I., Tsutsumi, Y., Sato, T., Koseki, J. Kuwano, R. (2007), "Small Strain Stiffness of Clean Sand And Gravel Based on Dynamic and Static Measurements", *Proc. of 9th IS Symposium*, JSCE, pp. 171-174.
- White, J. E. (1965). "Seismic Wave." McGraw-Hill Book Company, Inc., New York.
- Woods, R.D. (1991). "Field and Laboratory Determination of Soil Properties at Low and High Strains," *Proc. of 2nd Intl. Conf. on Recent Advances in Geotechnical Earthquake Eng. and Soil Dynamics*, pp. 1727-1741.